J Mater Sci (2011) 46:4308–4313
DOI 10.1007/s10853-011-5369-z

IIB 2010

Direct observation and quantification of grain boundary shear-migration coupling in polycrystalline Al

F. Mompiou · M. Legros · D. Caillard

Received: 25 August 2010 / Accepted: 3 February 2011 / Published online: 15 February 2011

Abstract Rapid grain boundary motion under stress has been observed during in-situ TEM straining experiment in polycrystalline Al at moderate temperatures. Crystallographic orientation of both sides of moving grain boundaries (GBs) was simultaneously recorded. A shear produced by the grain boundary migration has been estimated using fiducial markers and image correlation yielding a coupling factor (i.e., ratio of the shear strain over the migration distance) of around 7%. This result is compared to existing models based on shear coupled migration theories, and is discussed within the new Shear Migration Geometrical model (SMIG).

Introduction

Since they occupy an increasing volume fraction as the grain size is decreased, grain boundaries (GBs) can play a crucial role in mechanical properties of small grain metals. Plasticity mechanisms associated to GB motion can be of several kinds such as GB sliding, rotation, or migration. In recent experiments, combining micro-mechanical testing and post mortem TEM, it has been shown that the sole motion of GB in nanocrystalline (nc) aluminium can produce strain, providing an alternate deformation mode to dislocation mechanisms [1–3]. In these experiments, a clear correlation between a grain size increase and an increasing plastic strain was established. However, due to the small grain size, the precise orientations of the grains were not known. Conversely, macroscopic experiments performed on Al bicrystals at moderate temperatures have shown that a GB can migrate under a small load (below the elastic limit) and produce a shear strain that can be quantified by the so-called coupling factor (i.e., the ratio of the migration distance over the shear strain) [4]. These results show a good agreement with Cahn's model. However, recent in-situ TEM straining experiments have shown that GB migration under stress in Al polycrystals can lead to a much smaller coupling factor than expected from Cahn's model [5, 6]. A new Shear Migration Geometrical (SMIG) model has been proposed to account for this discrepancy [7, 8]. In this article, we report a new coupling mode observed during an in-situ TEM straining experiments in Al at moderate temperature. We show that this mode can be explained using the SMIG model, owing a large amount of atomic shuffling.

F. Mompiou (✉) · M. Legros · D. Caillard
CEMES-CNRS, 29, rue Marvig, 31055 Toulouse, France
e-mail: mompiou@cemes.fr

Experimental

UFG Aluminium with an initial mean grain size of about 800nm was produced by equal channel angular pressing (ECAP). In situ straining experiments were carried out in a JEOL 2010 microscope operated at 200 kV. Rectangular UFG samples were prepared by spark cutting and thinned down by electro-chemical polishing using a methanol solution with 33% of nitric acid at $T = -10$ °C. Grain boundary motion was monitored by means of DVD/HD recording using a video rate MEGAVIEW III camera.

Results

Grain boundary migration under stress

Figure 1 has been extracted from a video sequence shot at 350 °C inside the TEM. It shows an assembly of several

grains labelled Gi. At such temperature, recrystallization has already occurred leading to a larger grain size than in the initial structure (Fig. 1a). Note the presence of small defects labeled X which act as fiducial markers (markers contrast is enhanced). Under a uniaxial stress, directed along the direction T, the GB between G1 and G2 starts to move at a velocity of few hundred nm/s (Fig. 1b). Then it stops as soon as the local stress is fully relaxed and starts again as soon as an increment of stress is applied, confirming that the GB motion is stress driven. The trace indicating the initial position of the mobile GB (labelled tr) can be seen in Fig. 1b and also on the stereographic projection in Fig. 1c. This trace is due to thermal grooving at the sample surface. Although the GB plane cannot be exactly determined, its apparent width suggests that for a typical foil thickness of 500nm, it is inclined of 15° from the edge-on configuration. The different grain orientations have been determined. There are multiple equivalent descriptions of GB orientation relationship. We will choose to describe the GB as a $\langle 032 \rangle$ 126° GB for two reasons explained below. First, we expect that large tilt component GBs are favored, because they yield to a maximum shear strain. Indeed, the coupling factor varies as cos δ, where δ is the angle between the GB plane normal and the rotation axis. Since the GB plane is a plane close to the plane indicated with a dash line in Fig. 1c and contains the rotation axis $R = \langle 032 \rangle$, then the GB has a large tilt component in this description. Second, atomic shuffling required during the shear-migration process is supposed to be easier in dense plane. This implies for pure tilt GBs low-index GB rotation axes. The chosen description is the only one which fullfil these two conditions.

Determination of the coupling factor

Figure 2a is the result of the differential contrast between the images taken before (Fig. 1a) and after GB motion (Fig. 1b). The position of the two pictures has been adjusted in such a way that a maximum coincidence (e.g., minimum contrast intensity) is obtained at X1 (Fig. 2a). The migration distance ($d_\perp$) taken perpendicular to the GB plane is clearly shown (Fig. 2a). It appears then, that the images of the V-shape marker X2 in the adjacent shrinking grain do not superimpose. The arrows joining the marker before (in black) and after (in white) GB motion in Fig. 2 indicate the amplitude and the direction of the displacement projected in the plane of the figure. This can be explained by considering a coupling between stress and migration (over a distance $d_\perp$), producing a shear strain (i.e., a displacement $d_\parallel$ for a migration distance $d_\perp$) parallel to the interface, as schematically represented in Fig. 2b. The coupling factor, $\beta = d_\parallel / d_\perp$ can be directly measured on Fig. 2a. It is comprised between 7 and 8%. This value should be taken with caution because: (i) the displacement perpendicular to the specimen foil is unknown, and (ii) it is assumed that the measured shear is equal to the shear produced by an infinitely long GB, i.e., the other adjacent GBs (between G2 and G3, and between G2 and G4) do not restrain the shear.

Interpretation

Comparision with existing models

This coupling mode can be compared with existing theories of GB migration. Due to a high GB speed, long range diffusion processes can be ruled out. On the contrary, it is well known in displacive phase transformations that interfaces can move under stress at high speed without long range diffusion. Twinning is an example of such a shear-migration coupling. In fcc crystals, it occurs via the repeated nucleation and propagation of partial dislocations every atomic planes parallel to the interface, thus involving no diffusion. For coincident GB, it has been proposed that displacement shift complete (DSC) dislocations with associated steps can move repeatdly along the periodic plane GB in a step-wise manner in conjunction with a coordinated rearrangement of a large number of atoms [9]. However, this description cannot match the picture of polycrystalline materials were random orientations and high angle non-coincident GBs are usual features. Particular cases of the DSC dislocation theory can be found in the literature (see for instance [10–12]). The pure shuffling mode proposed by Babcock and Baluffi [13], corresponds to the case where the Burgers vector of DSC dislocation reduces to zero and the GB migrates without producing deformation.

Cahn's model [5, 6] which revivified an original work of Read and Shockley [14] is based on the idea that the concept of the motion of edge dislocations which constitute a small GB, can be extended to any large angle symmetrical tilt GB, their dislocation density being given by the Frank–Bilby equation [15, 16]. Because the dislocation density in the GB can vary continously, Cahn's model predicts, for $\langle 001 \rangle$ GBs, a coupling factor that varies continuously with the misorientation as $\beta = 2\tan(\theta/2)$ (1st coupling mode for $\theta < 90°$) and $\beta = 2\tan(\pi/4 - \theta/2)$ (2nd coupling mode for $\theta > 90°$). These two modes correspond, respectively, to the motion of 1/2 $\langle 110 \rangle$ and $\langle 100 \rangle$ dislocations with Burgers vectors both perpendicular to the GB plane and to the misorientation axis. Following this description, only [100] dislocations can move in the case of a $\langle 032 \rangle$ GB, leading to an expected coupling factor following $\beta = 2\tan(\pi/4 - \theta/2)$. This description leads to

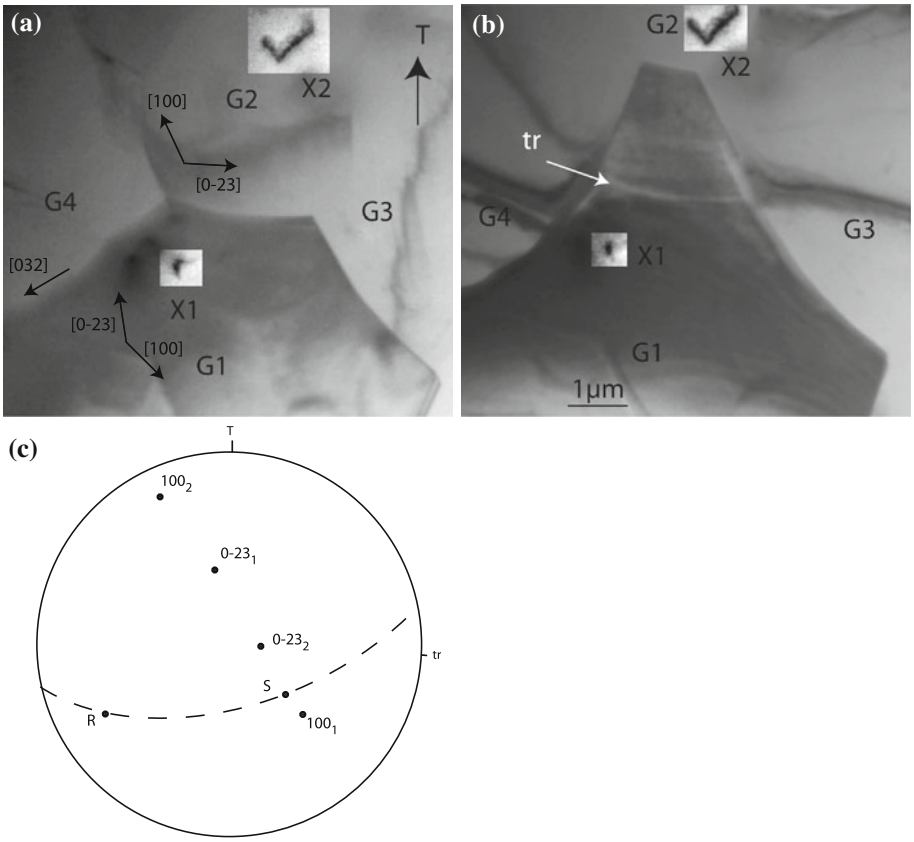

Fig. 1 **a–b**Stress assisted growth of grain G1 in polycrystalline Al at 350 °C. The trace (tr) left at the surface is typical of thermal grooving and indicates the initial position of the GB between G1 and G2. Note the presence of markers X1 and X2 attached to the sample surface. **c** The stereographic projection of the two grains

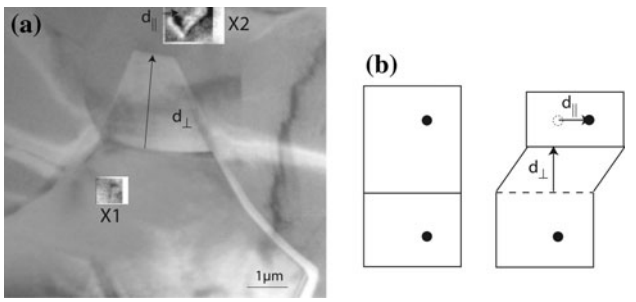

Fig. 2 **a** Differential image of pictures taken before (Fig. 1a) and after (Fig. 1b) GB motion. Images have been adjusted in order to superimpose the two images on marker X1. The GB migration distance ($d_\perp$) is indicated. Note that both images of X2 do not superimpose indicating that a deformation has occurred as sketched in **b**

large coupling factors (65% for $\theta = 126°$). This is clearly not in agreement with the result shown above. It can be argued that lattice dislocations which are supposed to compose the GB are meaningless as soon as the misorientation angle, which determines the dislocation spacing, is larger than around 15°. As pointed out by Cahn et al. [6], this contradiction can be overcome by considering alternatively as proposed in the DSC dislocation model that coupling occurs due to the lateral motion of step dislocations in the GB plane. Equivalence between the two descriptions is achieved for coincident GB by considering only two types of DSC dislocations, giving then two coupling modes. However, in the case of non-coincident GBs, the description should be extended to any kind of admissible defects. The concept of step-wise dislocation, as suggested by Pond [6], is then probably a more realistic description.

The SMIG model

The present model called SMIG model, can be viewed as an extension of Cahn's model to any kind of admissible defects that can be easily determined through a geometrical analysis. The main original idea is to consider the two adjacent grains as being two different phases, but having the same type of atoms and lattice volume. These two phases can be defined in the plane perpendicular to the GB plane and to the rotation axis by a set of two parallelogram motives (in the following labelled by subscripts 1 and 2), each of them being described by two vectors $\mathbf{u} = g\mathbf{i} + h\mathbf{j}$ and $\mathbf{v} = k\mathbf{i} + l\mathbf{j}$, g, h, k and l being integers and $\mathbf{i}$, $\mathbf{j}$ unit cell vectors in the plane perpendicular to the GB plane (Fig. 3).

Since we look for a diffusionless transformation (i.e., a pure shear parallel to the GB plane), the two

parallelograms are chosen with the same area and the same number of lattice sites N, i.e.,

$$N = \det(\mathbf{u_1}, \mathbf{v_1}) = \det(\mathbf{u_2}, \mathbf{v_2}) \quad (1)$$

The two parallelogram vectors can be defined in an orthonormal lattice :

$$\mathbf{u} = \begin{pmatrix} u_x \\ u_y \end{pmatrix} = P \begin{pmatrix} g \\ h \end{pmatrix}$$
$$\mathbf{v} = \begin{pmatrix} v_x \\ v_y \end{pmatrix} = P \begin{pmatrix} k \\ l \end{pmatrix} \quad (2)$$

with

$$P = \begin{pmatrix} r\sin\alpha & 0 \\ r\cos\alpha & 1 \end{pmatrix} \quad (3)$$

α being the angle between the lattice vectors $\mathbf{i}$ and $\mathbf{j}$ and $r = \|\mathbf{j}\|/\|\mathbf{i}\|$.

The SMIG model then consists in finding couples of shear and rotation values, able to transform one lattice orientation into another. This can be achieved by searching colinear vectors $\mathbf{d}_\parallel$ such that (see Fig. 4):

$$\mathbf{d_{u\parallel}} = R(\theta)\mathbf{u_2} - \mathbf{u_1} = K(R(\theta)\mathbf{v_2} - \mathbf{v_1}) = K\mathbf{d_{v\parallel}} \quad (4)$$

with $K = d_{u\perp}/d_{v\perp}$ and $R(\theta) = \begin{pmatrix} \cos\theta & -\sin\theta \\ \sin\theta & \cos\theta \end{pmatrix}$ the rotation matrix of the angle θ. The migration distance $d_\perp$ associated to the shear $d_\parallel$ is defined by:

$$d_{u\perp} = \mathbf{n} \cdot \mathbf{u_1}$$
$$d_{v\perp} = \mathbf{n} \cdot \mathbf{v_1} \quad (5)$$

where $\mathbf{n}$ is the unit vector normal to the GB plane. This imposes that

$$\det(\mathbf{d_{u\parallel}}, \mathbf{d_{v\parallel}}) = \det(R(\theta)\mathbf{u_2} - \mathbf{u_1}, R(\theta)\mathbf{v_2} - \mathbf{v_1}) = 0 \quad (6)$$

For a given set of two parallelogram motives the Eq. 4 admits two solutions for a misorientation angle θ given by:

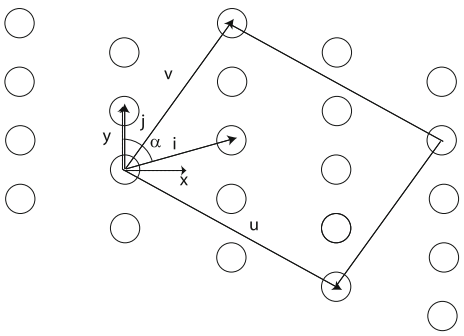

Fig. 3 Definition of vectors in the plane perpendicular to the GB plane. Here an example of the (032) plane with $\mathbf{i} = 1/2[1\bar{2}3]$ and $\mathbf{j} = [100]$. Parallelogramms are defined by $\mathbf{u}$ and $\mathbf{v}$ vectors which can be expressed in the orthogonal lattice ($\mathbf{x}$, $\mathbf{y}$)

$$\theta = 2\arctan\frac{B \pm C}{A} \quad (7)$$

with A, B, and C analytical functions given in the Appendix. The coupling factor is then given by:

$$\beta = \frac{d_{u\parallel}}{d_{u\perp}} = \frac{d_{v\parallel}}{d_{v\perp}} \quad (8)$$

It seems reasonnable to consider that shear coupled GB migration occurs sequentially by the nucleation and propagation of defects. From this geometrical model, it is tempting here to identify the vector $\mathbf{d}_\parallel$ to a DSC dislocation vector having a step character of height $h = d_\perp$. This is supposed to be the case for low index symmetric pure tilt coincident GB, where the most favorable GB plane is a low index periodic plane for the two crystals parallel to $\mathbf{d}_\parallel$. However, in the general case, the vector $\mathbf{d}_\parallel$ is not supposed to repeat periodically, or can repeat with a large period. In that case, it is then expected that a step-dislocation, called disconnection by Pond et al. [17], moves along the most favorable plane (called terrace), the alternance of terraces and steps following in average the GB plane. A large number of possible coupling factors can be computed using different sets of parallelegram motives. Crosses in Fig. 5 represent the possible coupling modes having a coupling factor β (less than 1 and for $N \leq 20$) as a function of the misorientation angle θ for a $\langle 032 \rangle$ GB (we take here $\mathbf{i} = [100]$, $\mathbf{j} = 1/2[1\bar{2}3]$ $r = \sqrt{14}/2$ and $\alpha = \arctan(1/\sqrt{14})$). For symmetry consideration, the misorientation angle is θ or $180 - \theta$, so that the abscissa of Fig. 5 can be restricted to the range $0° - 90°$.

The full line corresponds to the expected tangent rule $\beta = 2\arctan(\pi/4 - \theta/2)$ from Cahn's model considering edge dislocation of vector [100] gliding in a $(02\bar{3})$ plane. The grey area shows that close to $\theta = 54°$, several coupling modes are available with a coupling factor smaller than expected by Cahn's model.

A possible coupling mode that fits the experimental data is shown in Fig. 6. It corresponds to the mode indicated by an encircled cross in Fig. 5.

Fig. 4 In the SMIG model, the two set of vectors ($\mathbf{u}$, $\mathbf{v}$) defining the two initial parallelogram motives are related by a translation vectors $\mathbf{d}_\parallel$ such that $\mathbf{d_{u\parallel}} = R(\theta)\mathbf{u_2} - \mathbf{u_1} = K(R(\theta)\mathbf{v_2} - \mathbf{v_1}) = K\mathbf{d_{v\parallel}}$, with $K = d_{u\perp}/d_{v\perp}$ and θ the misorientation angle

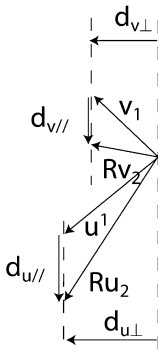

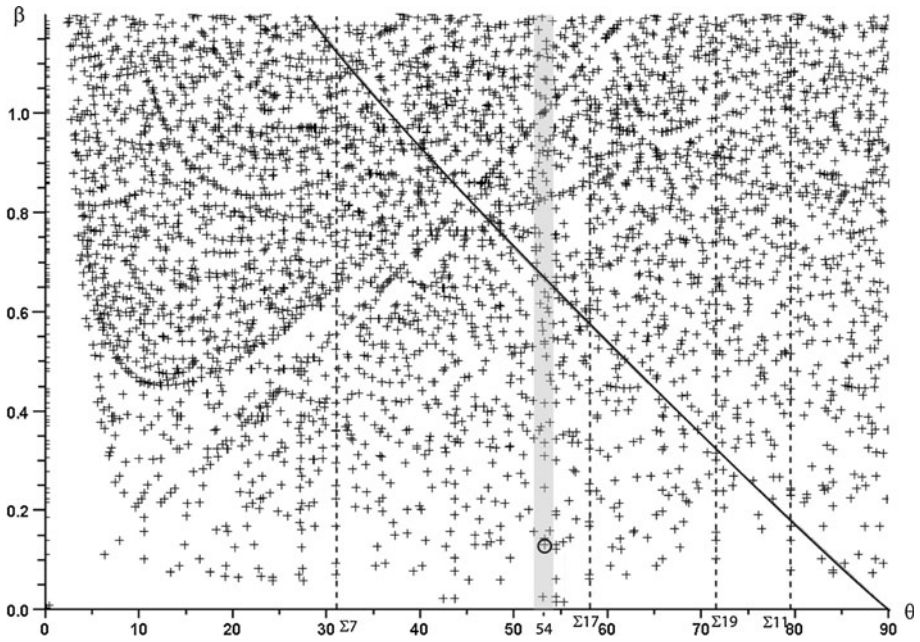

Fig. 5 Predicted coupling factors ($\beta < 1$ and $N < 20$) for a $\langle 032 \rangle$ GB as a function of the misorientation angle θ, for the SMIG model (*crosses*), and for Cahn's model (*full line*). Coupling modes expected for the observed GB shear coupled migration are located in the *grey area* close to $\theta = 54°$ (modulo 180°). The coupling mode indicated by the *encircled cross* is shown in Fig. 6

Two parallelograms (labelled 1 and 2) embedding $N = 10$ atoms are defined in the (032) plane (Fig. 6a). The parallelogram 2 is then rotated by an angle $\theta = 126.72°$, close to the misorientation angle. In that configuration, the two parallelograms can be deduced one from the other by a shear transformation (Fig. 6b). The shear direction $d_{\parallel}$ is indicated by arrows. It corresponds to the direction indicated in Fig. 1c contained in the mean GB plane. Figure 6b shows how the GB can possibly move. A step dislocation is nucleated and creates a step of height $d_{\perp}$ at an initial position *i*. The step is then moved along a terrace to *f*. Note that the terrace plane is not exactly parallel to the mean GB plane, i.e., $d_{\parallel}$ is not parallel to the terrace plane. In the meantime, atoms located in the grey area have been subjected to a shuffling from the black to the white positions. The number of shuffled atoms is $N - 1$. The corresponding coupling factor is equal to 13% in this case, close to the experimental value. We can see here that this mode requires a high number of shuffled atoms (9 atoms). When the number of shuffled atoms increases, step height increases and then coupling factors decrease. We can then expect a high activation energy for these low coupling modes. Low coupling modes are however required in polycrystals in order to minimize strain incompatibilities that can arise in the overall deformation process. This contrasts with the macroscopic deformation of bicrystals

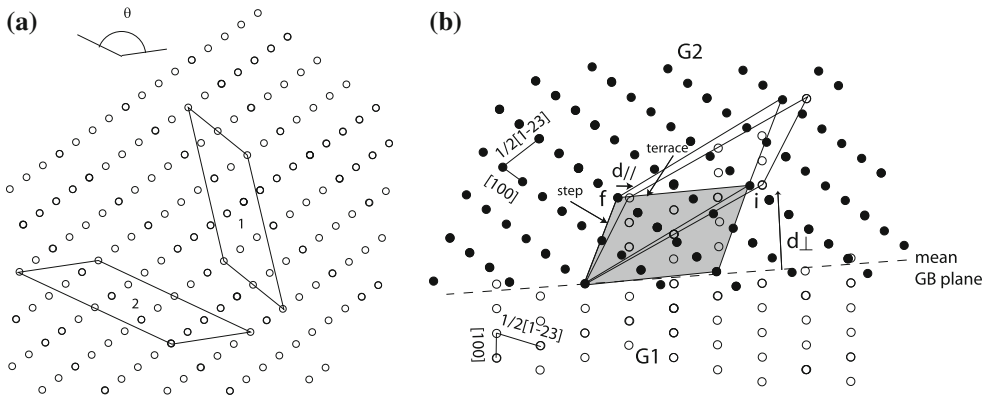

Fig. 6 Example of a shear migration coupling mode described with the SMIG model. This mode is found by defining two parallelograms in the plane perpendicular to the GB plane (**a**) related by a rotation (θ) and a shear transformation (*arrows*) (**b**). **b** The GB moves in this mode in a stepwise manner by creating a step-dislocation of Burgers vector $\mathbf{d}_{\parallel}$ gliding along terraces following a mean GB plane. This lateral motion between **i** and **f** involves a short range atomic rearrangement in the *grey area*

where both the geometry of the mechanical test and the microstructure would favor low activation energy, i.e., low number of shuffled atoms, and thus high coupling factors.

Conclusions

This work confirms that GB shear-migration coupling can carry plasticity. This plastic mechanism could prevail in confined media where dislocation nucleation is hindered. Here, we have reported an experimental measurement of a coupling factor (i.e., the produced shear strain) for a non-coincident GB that can be fitted with a coupling factor calculated using the SMIG model. This model is a general formulation of existing shear-coupled migration theory relying on step dislocation and short range atomic rearrangement. It allows a larger number of coupling factors (including low values), which are necessary to account for collective GB migration in real polycrystals. However, other parameters should be taken into account to describe properly GB coupled migration in a polycrystal. For instance triple line migration and GB migration under surface tension might result of different mechanisms involving only shuffling.

Appendix

$$A = (u_{1y} + u_{2y})(v_{1x} + v_{2x}) - (u_{1x} + u_{2x})(v_{1y} + v_{2y}) \quad (9)$$

$$B = u_{1x}v_{2x} + u_{1y}v_{2y} - u_{2x}v_{1x} - u_{2y}v_{1y} \quad (10)$$

$$C = \frac{1}{2}\big[4(u_{2x}v_{1x} + u_{2y}v_{1y} - u_{1x}v_{2x} - u_{1y}v_{2y})^2 - 4((u_{1y} - u_{2y})(v_{1x} - v_{2x}) - (u_{1x} - u_{2x})(v_{1y} - v_{2y})) \times ((u_{1y} + u_{2y})(v_{1x} + v_{2x}) - (u_{1x} + u_{2x})(v_{1y} + v_{2y}))\big]^{1/2} \quad (11)$$

References

1. Gianola DS, Van Petegem S, Legros M, Brandstetter S, Van Swygenhoven H, Hemker KJ (2006) Acta Materialia 54:2253
2. Legros M, Gianola DS, Hemker KJ (2008) Acta Mater 56:3380
3. Rupert TJ, Gianola DS, Gan Y, Hemker KJ (2009) Science 326:1686
4. Gorkaya T, Molodov D, Gottstein G (2009) Acta Mater 57(18): 5396
5. Cahn JW, Taylor JE (2004) Acta Mater. 52:4887
6. Cahn JW, Mishin Y, Suzuki A (2006) Acta Mater 54:4953
7. Caillard D, Legros M, Mompiou F (2009) Acta Mater 57:2390
8. Mompiou F, Legros M, Caillard D (2010) Acta Mater 58:3676
9. Rae CM, Smith DA (1980) Phil Mag A41:477
10. Babcock SE, Balluffi RW (1989) Acta Metall 37:2357
11. Fukutomi H, Iseki T, Endo T, Kamijo T (1991) Acta Metall Mater. 39:1445
12. Guilloppe M, Poirier JP (1980) Acta Metall 28:163
13. Babcock SE, Balluffi RW (1989) Acta Metall 37:2367–2376
14. Read WT, Shockley W (1957) Imperfections in nearly perfect crystals. Wiley, New York
15. Bilby BA (1955) Bristol conference report on defects in crystalline materials physical society, London
16. Franck FC (1950) Symposium on the plastic deformation of crystalline solids, Office of naval research
17. Pond RC, Ma X, Chai YW, Hirth JP (2007) Dislocations in solids. Elsevier, Amseterdam